

# 1 Description of System

We consider a system with a Lagrangian,

$$\mathcal{L} = \frac{1}{2}\phi(\square + m_\phi^2)\phi + \frac{\gamma}{2}\chi(\square + m_\chi^2)\chi + V(\phi, \chi). \quad (1)$$

Where  $\square = \partial_t - \nabla^2$  is the D'Alembertian operator,  $\nabla$  is a gradient,  $\phi$  and  $\chi$  are scalar fields, and  $V(\phi, \chi)$  is a nonlinear potential that couples the scalar fields. The ghost appears in this Lagrangian if the scalar fields are assigned oppositely signed kinetic energy terms,  $\gamma = -1$ .

We find the strong equations of motion

$$\square\phi + m_\phi^2\phi + \partial_\phi V = 0, \quad (2)$$

$$\square\chi + m_\chi^2\chi + \gamma\partial_\chi V = 0. \quad (3)$$

Since the original system is second order in time, it is ideal for the weak formulation to introduce auxiliary variables such that our system can be reduced to one that is first order in time.

Let  $u = \partial_t\phi$  and  $v = \partial_t\chi$ . From Eqns. 2 and 3, we have

$$\frac{\partial u}{\partial t} - \nabla^2\phi + m_\phi^2\phi + \frac{\partial V}{\partial\phi} = 0, \quad (4)$$

$$\frac{\partial\phi}{\partial t} - u = 0, \quad (5)$$

$$\frac{\partial v}{\partial t} - \nabla^2\chi + m_\chi^2\chi + \gamma\frac{\partial V}{\partial\chi} = 0, \quad (6)$$

$$\frac{\partial\chi}{\partial t} - v = 0. \quad (7)$$

# 2 Space-time FEM Formulation

An important step in any FEM is determining the element stiffness matrices. These matrices are found by solving the weak form of the equations of motion. Solving the space-time FEM for the 1+1 case results in 4x4 matrices, the 2+1 case finds 8x8 matrices, and the 3+1 case has 16x16 matrices.

The weak equations are 8, 9, 10, and 11 and we display them in their 1+1 form.

$$K_1 = \int_{X,T} (u_t\Psi + \phi_x\Psi_x + m_\phi^2\phi\Psi + V_\phi\Psi) dxdt \quad (8)$$

$$K_2 = \int_{X,T} (\phi_t\Psi - u\Psi) dxdt \quad (9)$$

$$G_1 = \int_{X,T} (v_t\Psi + \chi_x\Psi_x + m_\chi^2\chi\Psi + \gamma V_\chi\Psi) dxdt \quad (10)$$

$$G_2 = \int_{X,T} (\chi_t\Psi - v\Psi) dxdt \quad (11)$$

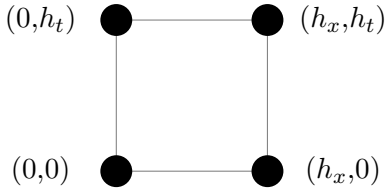
Recall that  $\Psi$  in the above equations is the test function. The test function is a piecewise polynomial function and can take on many different forms. For our purposes, a rectangular basis function is used. Once the rectangular element basis function is determined, it will be inserted into the weak equations. These integrals will be solved over each element and three 4x4 element stiffness matrices will be produced.

## 2.1 Element Basis Function

The rectangular element basis function is a piecewise polynomial with four terms,

$$\Psi_i(x, t) = b_{1,i}x + b_{2,i}t + b_{3,i}xt + b_{4,i}. \quad (12)$$

To solve for the unknown coefficients in Eq. 12, we consider the four corners of a rectangle in the  $(x, t)$  plane, see Fig. 2.1. In figure 2.1,  $h_x$  and  $h_t$  represent the step size. They can be thought of as the



distance between spatial and temporal nodes. They are defined by

$$h_x = \frac{x_{\text{final}} - x_{\text{initial}}}{n_x}$$

$$h_t = \frac{t_{\text{final}} - t_{\text{initial}}}{n_t - 1}$$

where  $n_x$  and  $n_t$  are the number of spatial and temporal nodes in the entire domain. Thus,  $n_x$  and  $n_t$  control the resolution of the simulation; as the number of nodes grows, the distance between nodes shrinks, and the domain becomes more refined. It should be noted that the  $(n_x)$  and  $(n_t - 1)$  terms in the denominators of the above equations is not a mistake. It must be this way since we implement periodic spatial boundaries but impose no such condition temporally.

Since we are currently looking for the element stiffness matrix, only one ‘element’ is examined in the entire domain. The element can be visualized as has been done in Fig. 2.1 with each corner representing a node designated by the subscript  $i$ . The coordinates  $(0, 0)$ ,  $(h_x, 0)$ ,  $(0, h_t)$ ,  $(h_x, h_t)$  will be inserted into Eq. 12 so that the  $b$  coefficients can be found. This results in four separate  $\Psi$  equations. To

determine the basis function, we require that

$$\Psi_i = \begin{cases} 1, & \text{if } j = i \\ 0, & \text{if } j \neq i \end{cases}$$

where  $j$  is represented as is described in Table 1.

Table 1: Representation of  $j$ .

$j$	$x$	$t$
1	0	0
2	0	$h_t$
3	$h_x$	0
4	$h_x$	$h_t$

This results in four polynomials, the element basis functions

$$\begin{aligned}\Psi_1 &= -\frac{1}{h_x}x - \frac{1}{h_t}t + \frac{1}{h_x h_t}xt + 1, \\ \Psi_2 &= \frac{1}{h_x}x - \frac{1}{h_x h_t}xt, \\ \Psi_3 &= \frac{1}{h_x h_t}xt, \\ \Psi_4 &= \frac{1}{h_t}t - \frac{1}{h_x h_t}xt.\end{aligned}$$

## 2.2 Element Stiffness Matrices

Now that we have the basis functions, the element stiffness matrices can be determined. We will explain the set up of the element stiffness matrices, display the matrices, and then discuss practical implementation into the simulation.

In the two dimensional (1+1) case, the weak form of the equations of motion, equations 8, 9, 10, and 11, are double integrals over one space-time element in the domain,

$$\begin{aligned}K_1 &= \int_0^{h_x} \int_0^{h_t} (u_t \Psi + \phi_x \Psi_x + m_\phi^2 \phi \Psi + V_\phi \Psi) dx dt \\ K_2 &= \int_0^{h_x} \int_0^{h_t} (\phi_t \Psi - u \Psi) dx dt \\ G_1 &= \int_0^{h_x} \int_0^{h_t} (v_t \Psi + \chi_x \Psi_x + m_\chi^2 \chi \Psi + \gamma V_\chi \Psi) dx dt \\ G_2 &= \int_0^{h_x} \int_0^{h_t} (\chi_t \Psi - v \Psi) dx dt\end{aligned}$$

For demonstration purposes, we will put together the element stiffness matrices pertaining to the three linear terms in the weak EOM. The linear terms are the ones that do not include contributions from  $V$  or its partial derivatives. This will result in three  $(4 \times 4)$  element stiffness matrices each of the form

$$A = \begin{bmatrix} a_{1,1} & a_{1,2} & a_{1,3} & a_{1,4} \\ a_{2,1} & a_{2,2} & a_{2,3} & a_{2,4} \\ a_{3,1} & a_{3,2} & a_{3,3} & a_{3,4} \\ a_{4,1} & a_{4,2} & a_{4,3} & a_{4,4} \end{bmatrix}.$$

The Time, Space, and Standard element stiffness matrices come from solving

$$\begin{aligned} \text{Time}_{i,j} &= \int_0^{h_t} \int_0^{h_x} \left( \frac{\partial \Psi_i}{\partial t} \Psi_j \right) dx dt \\ \text{Space}_{i,j} &= \int_0^{h_t} \int_0^{h_x} \left( \frac{\partial \Psi_i}{\partial x} \frac{\partial \Psi_j}{\partial x} \right) dx dt \\ \text{Standard}_{i,j} &= \int_0^{h_t} \int_0^{h_x} (\Psi_i \Psi_j) dx dt. \end{aligned}$$

Since these terms are linear in the weak EOM, we are able to calculate their element stiffness matrices one time. This can be done by hand, but we choose to utilize the SymPy package in Python that is capable of handling symbolic integration.

$$\text{Time} = \frac{h_x}{12} \begin{bmatrix} -2 & -1 & 1 & 2 \\ -1 & -2 & 2 & 1 \\ -1 & -2 & 2 & 1 \\ -2 & -1 & 1 & 2 \end{bmatrix},$$

$$\text{Space} = \frac{h_t}{6h_x} \begin{bmatrix} 2 & -2 & -1 & 1 \\ -2 & 2 & 1 & -1 \\ -1 & 1 & 2 & -2 \\ 1 & -1 & -2 & 2 \end{bmatrix},$$

$$\text{Mass} = \frac{h_t h_x}{36} \begin{bmatrix} 9 & 18 & 36 & 18 \\ 18 & 9 & 18 & 36 \\ 36 & 18 & 9 & 18 \\ 18 & 36 & 18 & 9 \end{bmatrix}.$$

These matrices are hard-coded into the simulation and saved once since they never change.

The nonlinear terms of the weak EOM must be dealt with a little differently, but the gist is the same. Instead of being able to find the element stiffness matrices once at the beginning of the simulation, we must use a Gaussian quadrature routine to approximate the integrals of the potential terms over each element. This is done inside the `FormResidual()` and `FormJacobian()` routines.

### 3 Method of Manufactured Solutions MMS

We consider the following coupled partial differential equations (PDEs) in 1+1 dimensions:

$$\phi_{tt} - \phi_{xx} + \phi + V_\phi(\phi, \chi) = 0, \quad (13)$$

$$\chi_{tt} - \chi_{xx} + \chi - V_\chi(\phi, \chi) = 0, \quad (14)$$

where the highly nonlinear potential terms are defined as

$$V_\phi(\phi, \chi) = -2\lambda \phi \frac{A}{B^{1.5}}$$

$$V_\chi(\phi, \chi) = 2\lambda \chi \frac{C}{B^{1.5}}$$

with

$$A = \phi^2 - \chi^2 + 1$$

$$B = (\phi^2 - \chi^2 - 1)^2 + 4\phi^2,$$

$$C = \phi^2 - \chi^2 - 1.$$

Here,  $\lambda$  is a parameter controlling the strength of the nonlinear potential. It is set to 1.0 for all testing in this section.

#### 3.1 Problem Setup and Goal

The aim of our numerical implementation is to solve equations (13)–(14) using a space–time finite element method (FEM) within PETSc with a nonlinear solver (SNES). The code uses a formulation in which each space–time node carries four degrees of freedom:

- $\phi(x, t)$  and an auxiliary field  $u(x, t)$ , which is related to the time derivative of  $\phi$ , and
- $\chi(x, t)$  and an auxiliary field  $v(x, t)$ , which is related to the time derivative of  $\chi$ .

To verify our implementation, we use the *method of manufactured solutions* (MMS). The idea behind MMS is to choose a smooth (and nontrivial) manufactured solution for  $\phi(x, t)$  and  $\chi(x, t)$ , compute all

the required derivatives, and then add appropriate forcing functions so that the manufactured solution exactly satisfies the modified PDEs. In our case, we modify the equations to

$$\phi_{tt} - \phi_{xx} + \phi + V_\phi(\phi, \chi) = F_\phi(x, t), \quad (15)$$

$$\chi_{tt} - \chi_{xx} + \chi - V_\chi(\phi, \chi) = F_\chi(x, t). \quad (16)$$

The goal is to compute these forcing functions for  $\phi$  and  $\chi$  ( $F_\phi$  and  $F_\chi$ ) so that when the manufactured solution is substituted into the left-hand side of (15) and (16), the LHS exactly matches  $F_\phi(x, t)$  and  $F_\chi(x, t)$ .

### 3.1.1 Manufactured Solution

We choose the following manufactured solutions:

$$\phi(x, t) = 1 + \cos(\pi x) \cos(\pi t), \quad (17)$$

$$\chi(x, t) = 1 + \cos(\pi x) \sin(\pi t). \quad (18)$$

These functions are chosen because they are smooth, nontrivial, and spatially periodic on symmetric spatial domains.

### 3.1.2 Derivatives of the Manufactured Solution

Beginning with  $\phi(x, t)$  the first and second derivatives of the manufactured solution with respect to time are:

$$\begin{aligned} \phi_t(x, t) &= \frac{\partial}{\partial t} [1 + \cos(\pi x) \cos(\pi t)] = -\pi \cos(\pi x) \sin(\pi t), \\ \phi_{tt}(x, t) &= \frac{\partial}{\partial t} [-\pi \cos(\pi x) \sin(\pi t)] = -\pi^2 \cos(\pi x) \cos(\pi t). \end{aligned}$$

Similarly, the spatial derivatives are:

$$\begin{aligned} \phi_x(x, t) &= \frac{\partial}{\partial x} [1 + \cos(\pi x) \cos(\pi t)] = -\pi \sin(\pi x) \cos(\pi t), \\ \phi_{xx}(x, t) &= -\pi^2 \cos(\pi x) \cos(\pi t). \end{aligned}$$

Thus, we observe that

$$\phi_{tt} - \phi_{xx} = -\pi^2 \cos(\pi x) \cos(\pi t) - [-\pi^2 \cos(\pi x) \cos(\pi t)] = 0.$$

Therefore, the left-hand side of the  $\phi$ -equation (15) becomes

$$\phi + V_\phi.$$

Computing the time derivatives for  $\chi(x, t)$ :

$$\begin{aligned}\chi_t(x, t) &= \frac{\partial}{\partial t} [1 + \cos(\pi x) \sin(\pi t)] = \pi \cos(\pi x) \cos(\pi t), \\ \chi_{tt}(x, t) &= -\pi^2 \cos(\pi x) \sin(\pi t).\end{aligned}$$

And the spatial derivatives:

$$\begin{aligned}\chi_x(x, t) &= \frac{\partial}{\partial x} [1 + \cos(\pi x) \sin(\pi t)] = -\pi \sin(\pi x) \sin(\pi t), \\ \chi_{xx}(x, t) &= -\pi^2 \cos(\pi x) \sin(\pi t).\end{aligned}$$

Thus,

$$\chi_{tt} - \chi_{xx} = -\pi^2 \cos(\pi x) \sin(\pi t) - [-\pi^2 \cos(\pi x) \sin(\pi t)] = 0.$$

The left-hand side of the  $\chi$ -equation (16) then becomes

$$\chi - V_\chi.$$

### 3.1.3 Forcing Functions

Thus, we define the forcing functions as:

$$F_\phi(x, t) = \phi(x, t) + V_\phi(\phi(x, t), \chi(x, t)), \quad (19)$$

$$F_\chi(x, t) = \chi(x, t) - V_\chi(\phi(x, t), \chi(x, t)). \quad (20)$$

With these definitions, the modified (forced) problem becomes:

$$\phi_{tt} - \phi_{xx} + \phi + V_\phi(\phi, \chi) = F_\phi(x, t), \quad (21)$$

$$\chi_{tt} - \chi_{xx} + \chi - V_\chi(\phi, \chi) = F_\chi(x, t). \quad (22)$$

By construction, substituting the manufactured solutions (17) and (18) into the left-hand sides of (21) and (22) yields exactly  $F_\phi(x, t)$  and  $F_\chi(x, t)$ , respectively.

This recast's our weak EOM:

$$\begin{aligned}K_1 &= \int \left( \frac{\partial u}{\partial t} \Psi + \frac{\partial \phi}{\partial x} \frac{\partial \Psi}{\partial x} + m_\phi^2 \phi \Psi + \frac{\partial}{\partial \phi} V(\phi, \chi) \Psi - F_\phi \Psi \right) \\ K_2 &= \int \left( \frac{\partial \phi}{\partial t} \Psi - u \Psi \right) \\ G_1 &= \int \left( \frac{\partial v}{\partial t} \Psi + \frac{\partial \chi}{\partial x} \frac{\partial \Psi}{\partial x} + m_\chi^2 \chi \Psi - \frac{\partial}{\partial \chi} V(\phi, \chi) \Psi - F_\chi \Psi \right) \\ G_2 &= \int \left( \frac{\partial \chi}{\partial t} \Psi - v \Psi \right)\end{aligned}$$

By incorporating the forcing functions into the numerical solver, we can compute numerical solutions and compare them to the exact manufactured solutions. A convergence study is shown in table 2 which indicates 2nd order convergence.

### 3.1.4 Results

Table 2: Convergence Study Results

Mesh ( $nx \times nt$ )	$\phi L_2$ Error	Rate $_{\phi}$	$\chi L_2$ Error	Rate $_{\chi}$
$100 \times 101$	7.64e-04	-	9.08e-04	-
$200 \times 201$	1.90e-04	2.0037	2.26e-04	2.0049
$400 \times 401$	4.76e-05	2.0018	5.65e-05	2.0023
$800 \times 801$	1.19e-05	2.0008	1.41e-05	2.0011

The rates in table 2 are calculated by doing

$$Rate_{\phi/\chi} = \frac{\log(E_{coarse}/E_{fine})}{\log(h_{coarse}/h_{fine})}.$$

The mesh is setup up so that  $h = h_x = h_t$ . Thus,  $\log(h_{coarse}/h_{fine}) = \log(2)$ .

We see from figure 1 and table 2 that the numerical results compare nicely with the manufactured results. These findings give us good reason to believe that our 1+1 numerical implementation is working properly.

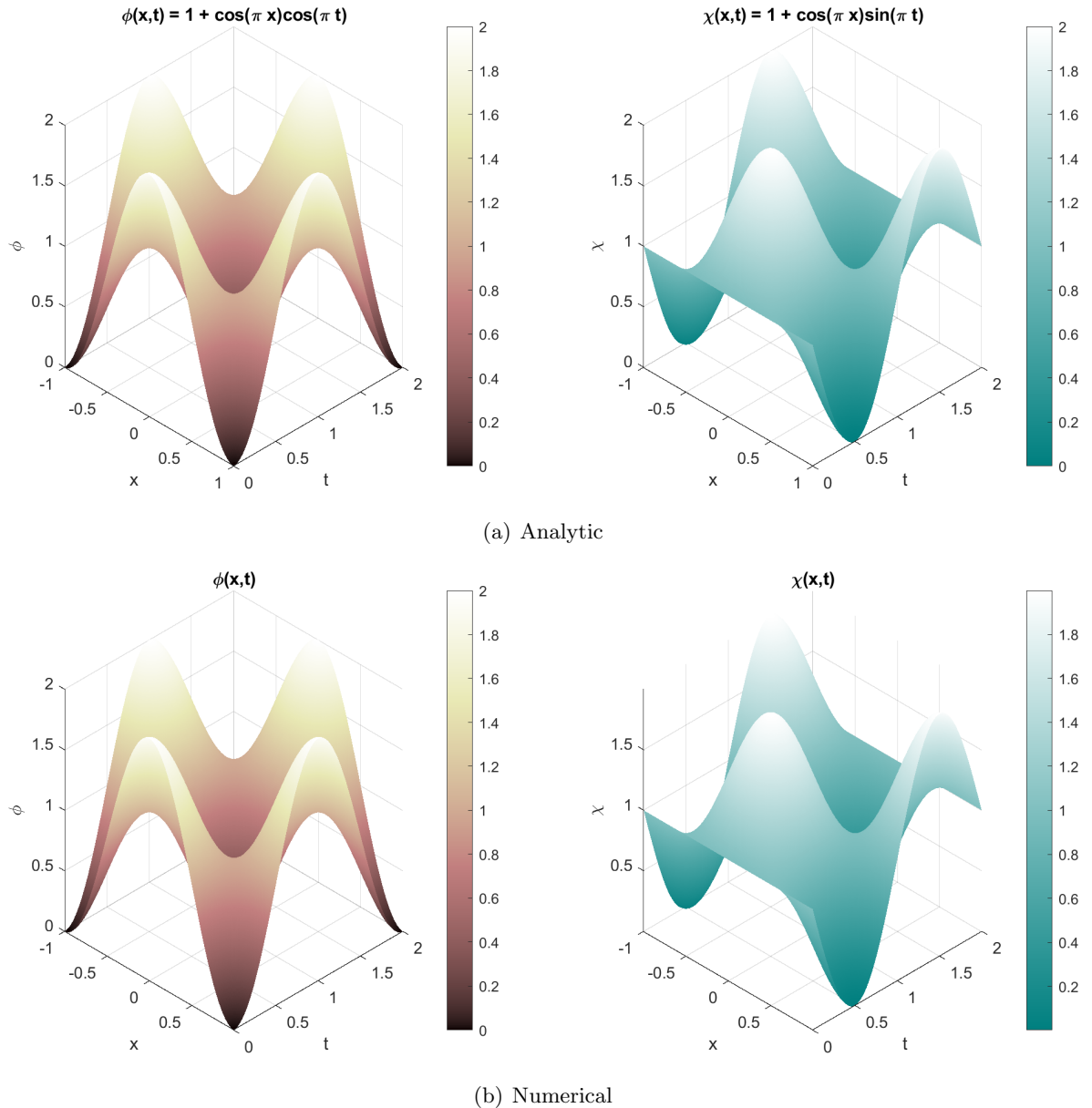


Figure 1: Comparison of 3D space–time surface plots for the analytic and numerical solutions. Both visualizations show  $\phi(x, t)$  and  $\chi(x, t)$  as functions of  $x$  and  $t$ .